

Acoustic backscattering by Hawaiian lutjanid snappers.

II. Broadband temporal and spectral structure

Whitlow W. L. Au^{a)} and Kelly J. Benoit-Bird

Hawaii Institute of Marine Biology, P.O. Box 1106, Kailua, Hawaii 96734

(Received 13 September 2002; accepted for publication 11 August 2003)

The characteristics of acoustic echoes from six species of deep-dwelling (up to 400 m) Hawaiian Lutjanid snappers were determined by backscatter measurements at the surface. A broadband linear frequency-modulated signal and a short dolphinlike sonar signal were used as the incident signals. The fish were anesthetized and attached to a monofilament net that was attached to a rotor so echoes could be collected along the roll, tilt, and lateral axes of each fish. The temporal highlight structure of broadband echoes was determined by calculating the envelope of the cross-correlation function between the incident signal and the echoes. The echo waveforms were complex with many highlights and varied with the orientation of the fish. In the tilt plane, the strongest echoes occurred when the incident signal was perpendicular to the long axis of the swimbladder. The number of highlights was the fewest at this orientation. The number of echo highlights and the length of echoes increased as the fish was tilted from this orientation. The highlight structure of the echoes resulted in the transfer function being rippled, with local maxima and minima that changed with fish size and species. The echo structures in both the time and frequency domains were generally consistent within species and were easily distinguishable between species. © 2003 Acoustical Society of America. [DOI: 10.1121/1.1614257]

PACS numbers: 43.30.Sf [WMC]

Pages: 2767–2774

I. INTRODUCTION

Information on the behavior, movement patterns, habitat utilization, and abundance of deepwater lutjanid snappers in Hawaii, an important and threatened fishery, is extremely limited (Haight *et al.*, 1993). Various acoustic techniques have the potential to provide important information to fill these gaps (MacLennan, 1990; MacLennan and Holliday, 1996; MacLennan and Simmonds, 1992; Simmonds and MacLennan, 1996). However, the difficulties identifying and estimating the abundance of species with acoustics limits the utilization of these techniques.

In order to identify species using acoustics, more information is required than can be obtained from a single frequency. Multiple-frequency techniques have been suggested as an effective way to estimate the size distributions and total abundance of many classes of organisms in the ocean (see a review in Greenlaw and Johnson, 1983). These methods have primarily been limited to discrete frequencies that must be carefully selected with knowledge of the scattering characteristics of potential targets.

Broadband acoustic signals, those that contain a continuous, wide range of frequencies rather than a few, discrete frequencies, have the potential to provide significant information about targets (Barr, 2001; Burdic, 1968). Species may reflect a broadband acoustic signal differently and these echo differences may be obvious in the time or frequency domains (Zakharia *et al.*, 1996). For example, differences may result in target strengths at specific frequencies; the number, position, and amplitude of echo highlights or spectral ripples as well as changes in these characteristics as a function of the

orientation of the target (Au and Snyder, 1980; Urick, 1983). Using a sonar with a broadband signal that has a good frequency and temporal resolution, the backscatter characteristics of different species may be resolvable.

In order to identify fish in the wild, however, information is needed on the characteristics of the population of interest and the relationship of these characteristics to the acoustic properties of the target populations. A mathematical or theoretical solution to this problem, particularly for complicated, acoustically understudied targets such as fish, is not currently available. The objectives of Part II of this work were to (1) determine if species-specific differences in the broadband characteristics of closely related Hawaiian lutjanid snappers exist; (2) quantify these differences; and (3) determine how these differences are affected by fish size. Three specific species of lutjanid snappers are of prime interest, the onaga or long-tailed red snapper (*Etelis coruscans*), the ehū or red snapper (*Etelis carbunculus*), and the opakapaka or pink snapper (*Pristipomoides filamentosus*). These three species are the most critical to the lutjanid fishery (Western Pacific Regional Fisheries Management Council, 1999) and are the most depleted in the main Hawaiian Islands.

II. METHODS

Acoustic data were collected as in Part I of this work (Benoit-Bird *et al.*, 2003a). Lutjanid snappers caught off the coasts of the Hawaiian Islands were allowed to acclimate to ambient conditions for at least eight days before their backscattering properties were measured. Although these lutjanid snappers are deep dwelling (up to 400 m), backscatter measurements done both at the surface and *in situ* at 250 m indicate that once the fishes acclimatize to surface condi-

^{a)}Electronic mail: wau@hawaii.edu

tions, their swimbladders retain a similar shape and volume as in deep waters (Benoit-Bird *et al.*, 2002). Live individual fish were anesthetized with 1 mL of 2-phenoxy-ethanol per 10 L of seawater and enclosed in a fitted bag made of monofilament netting. The net bag was mounted to a large, weighted, monofilament net that was turned by a rotor 360°.

Two broadband signals were used to measure backscattering; a frequency-modulated sweep with a frequency range of 60 to 200 kHz, and a dolphinlike click with a peak frequency of 120 kHz and a 60-kHz bandwidth. The ratio of fish length to acoustic wavelength at the peak frequency of the dolphinlike signal varied from 12 to 38, placing the results in the intermediate frequency range, where the swimbladder accounts for 90% to 95% of the reflected energy (Foote and Ona, 1985). The waveform and frequency spectrum of the signals are shown in Fig. 2 of Benoit-Bird *et al.* (2003a). The results from the dolphinlike signal were considered for time-domain analyses. The short duration of this signal (80 μ s) compared to the FM signal (500 μ s) made the highlight or echo structure more apparent without any special processing; however, the results with both signals are very similar after cross-correlating the echoes with the transmitted signal. For spectral domain analyses, the results from the frequency-modulated sweep were utilized because they included a slightly wider frequency range. Again, the results from the transfer functions of the two signals were similar above 75 kHz.

The outgoing signals were produced using a function generator computer plug-in board. The function generator also produced a trigger signal for each transmission. After a delay related to the two-way travel time from the signal to the target, a trigger prompted a Rapid System R1200 analog-to-digital (A/D) converter to digitize and store a block of 1024 samples. Sampling rates of 1 MHz were used for the function generator and the A/D converter. The delayed trigger also caused the rotor and net to advance by an incremental angle. Echoes were collected in 1.5°–2.5° increments about each of the fish's three axes for both source signals. The transmit and receive transducers, with an effective 12° 3-dB beamwidth at the center frequency of the signals, were set up 2.2 m deep, the same depth as the mounted fish, approximately 6 m from the fish. The use of broadband signals virtually eliminates the presence of side lobes (Au, 1993). After acoustic measurement, fish were sacrificed with a 2-mL/10-L dose of 2-phenoxy-ethanol. The standard length, total length, displacement volume, and wet weight of each fish were measured and the fish was immediately frozen.

A. Data analysis

The incident signals were measured and digitized with the receiving hydrophone located at the position of a target fish, directly facing the projecting transducer. Reflected signals were compared with the incident signals and corrected for gain. The envelope of the cross correlation between each echo and the incident signal were examined to determine their basic time-domain characteristics. The cross-correlation function was determined by the Fourier transform technique using the equation

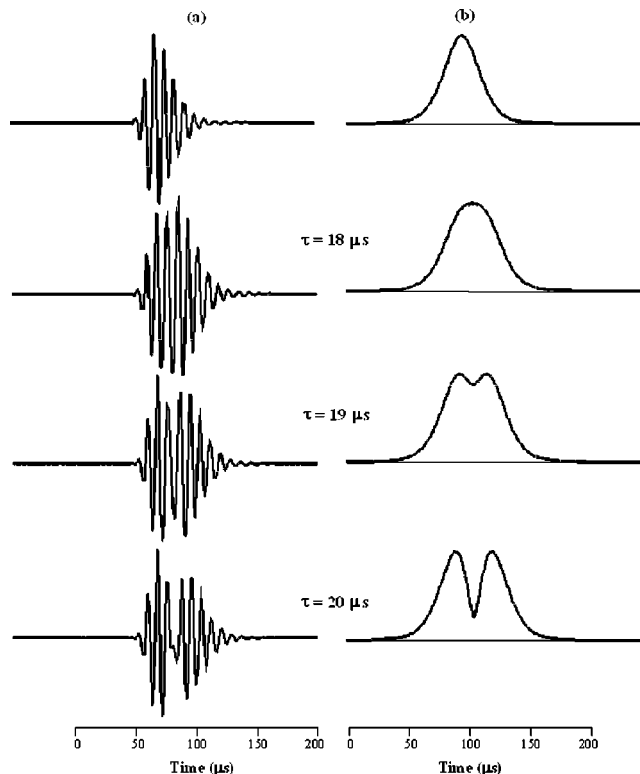


FIG. 1. The top left-hand panel is the waveform of the transmitted dolphinlike signal with the envelope of its auto-correlation function to the right. The remaining panels are simulated echoes consisting of the sum of two of the transmitted signal separated by a time τ (left) along with the envelopes of the cross-correlation functions between the transmitted signal and the simulated echoes (right). This figure shows the time-resolution property of signal.

$$c(t) = \mathcal{F}^{-1}[E(f)U(f)] \quad (1)$$

(Brigham, 1988) where $E(f)$ and $U(f)$ are the Fourier transform of the echo and incident signals, respectively, and \mathcal{F}^{-1} denotes the inverse Fourier transform of the terms in the brackets. The envelope of the cross-correlation function was calculated by converting $c(t)$ into an analytic signal using the Hilbert transform method where the absolute value of the analytic signal represents the envelope of the signal (Barr, 2001; Burdic, 1968).

The time resolution capability of the dolphinlike signal can be determined by simulating reflections from two discrete point targets separated by a travel time of τ as expressed by the equation

$$e(t) = s(t) + s(t - \tau), \quad (2)$$

where $s(t)$ is the incident signal that is reflected perfectly and $s(t - \tau)$ is another reflection delayed by a time τ . The result of this simulation is in Fig. 1, where the waveforms are under column **a**, and under column **b** are the envelopes of the cross-correlation functions. The first signal in column **a** is the incident signal, followed by signals described by Eq. (2) with various values of τ . The envelopes under column **b** in Fig. 1 indicate that highlights must be separated by at least 19 μ s before they are resolvable. Note that for $\tau=18$ the two highlights are not resolvable and the envelope of the cross-correlation function is wider than for the incident signal. This property and the 3-dB width of the correlation function (22 μ s) can be used to indicate whether a second highlight might

be hidden or unresolvable at different portions of an echo. The number of highlights, or glints, in each echo waveform was analyzed for each angle within 15° of the dorsal aspect, in both the tilt and roll planes.

Other characteristics of the waveforms were analyzed for echoes obtained from the dorsal aspect of each fish and at the tilt angle where maximum echo strength was measured. These characteristics, the relative amplitude of each highlight, the distance between highlight peaks, and the 3-dB width of each highlight, were compared between species, sizes, and angles.

The transfer function of dorsal aspect frequency-modulated echoes was determined using the equation

$$H(f) = 20 \log \left| \frac{E(f)}{U(f)} \right|. \quad (3)$$

The transfer function is characterized by an intricate spectrum with many peaks and nulls. Nulls were defined as decreases in echo intensity from the intensity at surrounding frequencies by at least 10 dB. Peaks were put into two categories, frequencies at which the intensity was 5 dB greater than surrounding intensities and those with 10 dB greater intensities.

III. RESULTS

The results are presented from the perspective of a broadband sonar pointed vertically downward. The waveforms of dorsal aspect echoes for the different species are shown in Fig. 2. The envelope of the cross-correlation function for each echo is represented by the dashed curve. From the time representation of the echoes, it is obvious that echo structures are very different between the species and that many highlights exist for most of the echoes. The echo structure is very complex with portions within echoes where two or more unresolvable highlights are apparently present. These are indicated by the width of the cross correlation function and the many oscillations of the signal within the wide correlation peaks. The echo structure obtained from 10–11 of each of the targeted or primary species were similar except for the highlight intervals which were somewhat related to fish size. The relationship between echo highlight intervals for highlights 2–8 and fish size for dorsal aspect echoes are plotted in Fig. 3. Some of the intervals changed significantly with fish size while others showed little change.

An example of the backscattered waveforms from a pink snapper as a function of the fish tilt angle is shown in Fig. 4. The lateral aspect x ray of the fish is shown with the tilt angles above each waveform indicating the orientation of the fish with respect to the direction of the sonar signal. At the 0° tilt angle, the longitudinal axis of the fish is perpendicular to the direction of the sonar signal. Each waveform is 500 μs in duration. The shape and orientation of the swimbladder with respect to the direction of the incident signal were the most important factors influencing the backscattered waveforms. The waveforms varied considerably as a function of the tilt angle with the most highlights present at the 15° and 10°

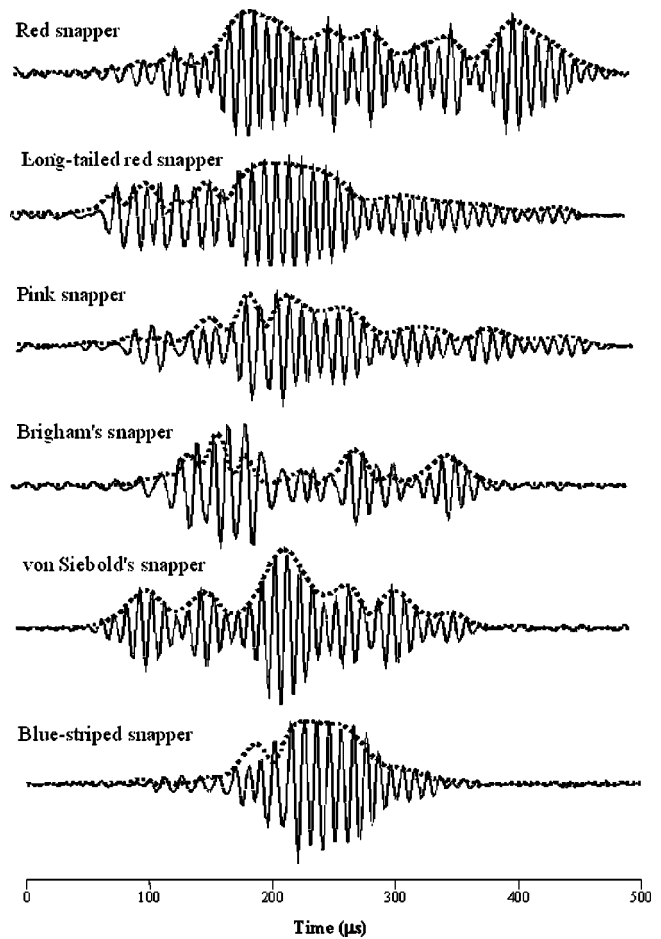


FIG. 2. Representative echoes from the dorsal aspect of six species of lutjanid snappers. The dashed line plotted with each echo is the envelopes of the cross-correlation function of the echo with the transmitted signal.

angles. The backscatter has the highest amplitude when the longitudinal axis of the swimbladder was approximately perpendicular to the sonar beam.

The number of echo highlights as a function of the tilt angle is shown in Fig. 5. The number of highlights varies with the tilt angle of the fish and is the least when the echo is the strongest. The echo is the strongest when the incident signal is perpendicular to the longitudinal axis of the swimbladder (Benoit-Bird *et al.*, 2003a). In all species, the number of highlights generally increases as the fish is tilted further from this point with the number of highlights gradually increasing towards increasing head-up aspect angle. The relative amplitude, interhighlight interval, and 3-dB width of the highlights for the three target species at the dorsal aspect and at the aspect at which the longitudinal axis of the swimbladder is perpendicular to the incident signal are shown in Fig. 6. All three of the parameters of Fig. 6 differed between different species.

It was not within the scope of this study to determine possible sources of reflections for the different highlights in a species. Considerably more knowledge on the scattering processes involved with a fish body, bony structures, and swimbladder shape and volume are required in order to determine the origin of the various highlights in an echo. Figure 7 illustrates the complexity of the task of identifying the sources

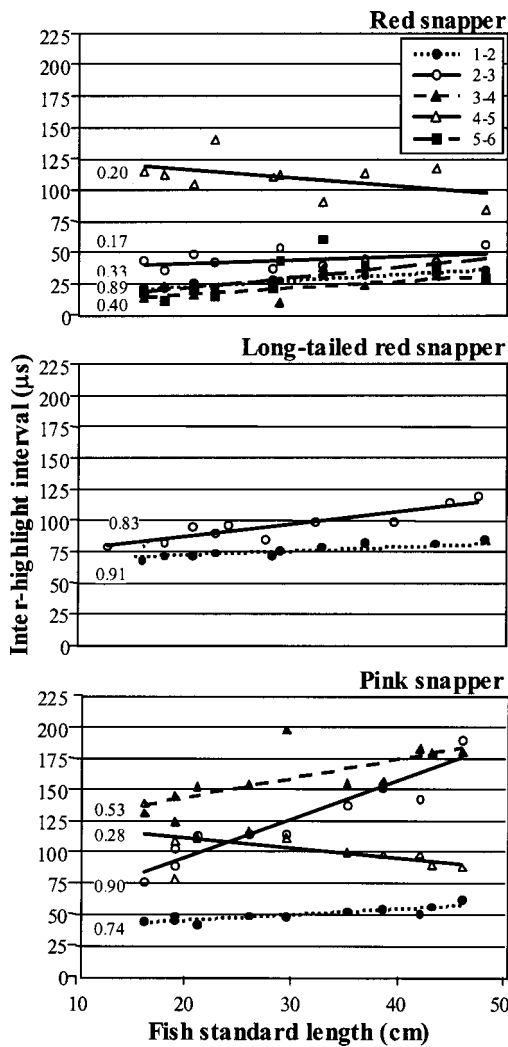


FIG. 3. The interval between each echo highlight as a function of fish length. Regression coefficients are shown for each relationship. Most intervals increased with increasing fish size, although some remained constant or decreased.

of highlights, showing the envelope of the cross-correlation function and an x ray of the corresponding fish (pink snapper). The relative time of occurrence of each highlight with respect to the first reflected component of the echo is shown in a table within the figure. Also shown is the two-way distance in cm that an acoustic signal would travel for the corresponding delay time. If we assume that the first highlight originated at the fish body, then the second highlight at $22 \mu\text{s}$ might have been from the forward tip of the swimbladder. After this simple explanation for the first two highlights, the situation becomes extremely complex, with two-way delay distances as large as 27.5 cm . The interhighlight interval plot of Fig. 6 also suggests relatively long echo structures that are not easily explainable. Furthermore, the width of most of the peaks of the cross-correlation function shown in Fig. 6 are greater than $22 \mu\text{s}$, suggesting that these highlights are composed of several unresolvable highlights.

As with target strength (Benoit-Bird *et al.*, 2003a), changes in echo structure were significantly reduced in the roll plane compared with the tilt plane. There were no significant changes in the number of echo highlights within 10°

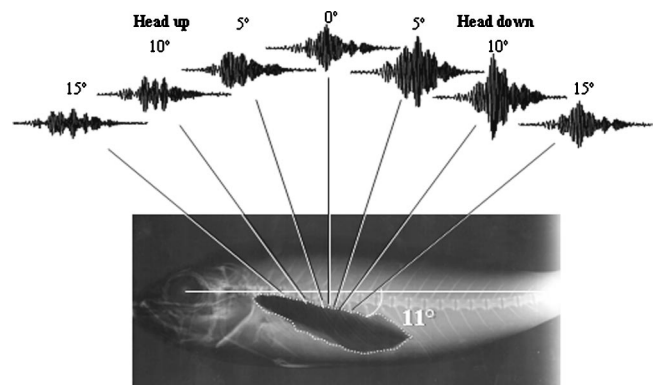


FIG. 4. An example of the echo waveforms from different tilt angles about the dorsal aspect of a pink snapper. The duration of each waveform is $500 \mu\text{s}$.

of fish dorsal aspect in the roll plane. The number of highlights increased by one in the long-tailed red snapper and pink snapper at 15° from dorsal and two in the red snapper. There were also few differences in the highlight structure, in terms of relative amplitude and width, over this range of roll angles. The 95% confidence intervals of all highlight characteristics measured at dorsal and 15° in the roll plane overlapped. Consequently, few differences were observed in the transfer functions (the spectral domain) as a function of roll angle.

The transfer functions of the dorsal aspect echoes were similar from both incident signal types. Because the frequency-modulated signal included a slightly wider frequency range, the echoes from this signal are presented. Species-specific differences in the spectral structure of broadband echoes are evident in Fig. 8. Because spectral and temporal structure are related, differences observed in the highlight structure as a function of orientation were mirrored in the spectra. The most conserved feature of spectral structure is the frequency position of nulls, sharp decreases in intensity of at least 10 dB , whose positions are associated with the interhighlight intervals in the time domain echoes.

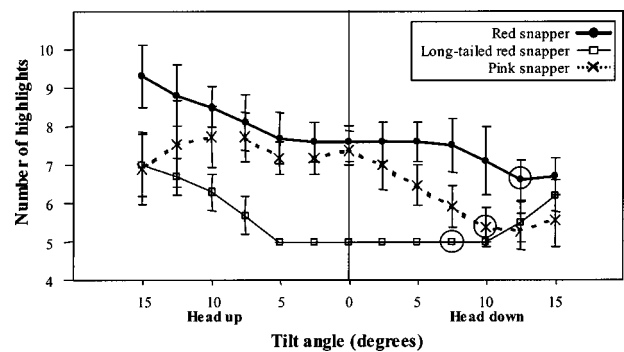


FIG. 5. The number of echo highlights, measured from the envelope of the cross-correlation between the echo and the incident signal as a function of fish tilt angle. The angle at which the strongest echo was obtained is circled. For each species, the number of highlights was the fewest at and around the angle at which the strongest echo was obtained. Error bars indicate one standard deviation.

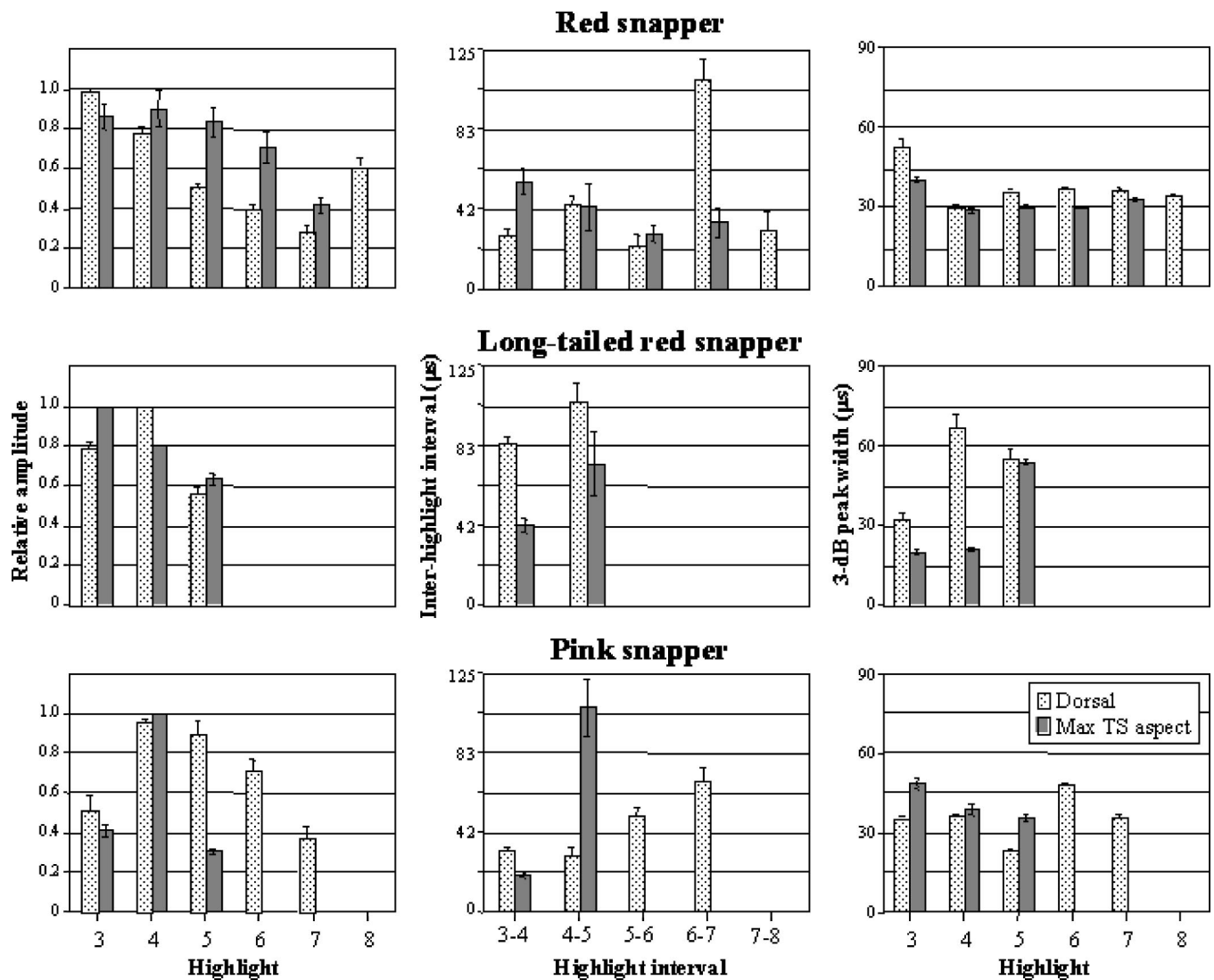


FIG. 6. Relative amplitude of each highlight (left), interval between each highlight peak (center), and the 3-dB width of each highlight (right) for each of the three primary species. Each characteristic is shown for dorsal aspect echoes, light gray, and the maximum amplitude dorsal echoes, dark gray. Error bars show 95% confidence intervals.

The position of spectral nulls was strongly related to fish size as seen in Fig. 9. The shift of the frequencies of spectral peaks and nulls as a function of fish length (L_F) was not constant as L_F/λ , where λ is wavelength. An analysis of variance revealed that there was still a significant effect of length on the position of spectral features after L_F/λ was considered ($p < 0.05$). However, when the length of the axes of the swimbladder (L_{SB}) was used, the position of spectral features that varied significantly as a function of length did not vary significantly as a function of L_{SB}/λ ($p > 0.05$ for all comparisons). This was particularly evident in the red snapper where swimbladder size and fish length are not as strongly correlated as in other species.

IV. DISCUSSION AND CONCLUSIONS

Echo highlight structure varied between fish species. While there was strong overlap in some highlight characters, in particular, the relative amplitude of highlights, when all three characters measured are utilized in concert, species differentiation is possible from echo highlight characters.

Within each species, the number of highlights in echo waveforms increased off-axis. The further each fish was tilted from its dorsal maximum target strength aspect, the greater the number of echo highlights. The length of the echo also increased off-axis. The shortest echo was observed in the highest amplitude echo. Roll plane changes in echo highlights were much smaller than those in the tilt plane. While the time-domain characteristics of echoes changed with aspect, the variance in these characteristics was much less within species than between them within $\pm 15^\circ$ about the dorsal aspect.

Species-specific differences in broadband echo characteristics were also visible in the spectral domain. The number of peaks and nulls, their position, relative amplitude, and width varied strongly between species. The position of peaks and nulls changed with fish size but the relative position and width of features did not change with fish size within a species. Few spectral characters were observed below about 100 kHz, regardless of fish size. This indicates that even low-frequency broadband echoes do not have the resolution to

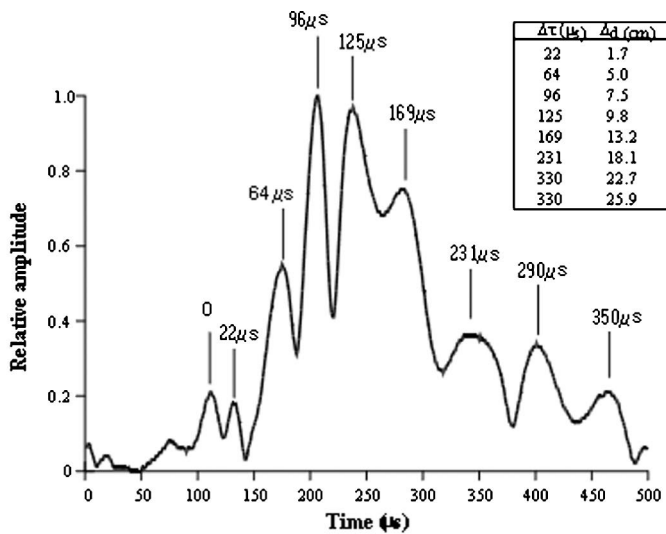
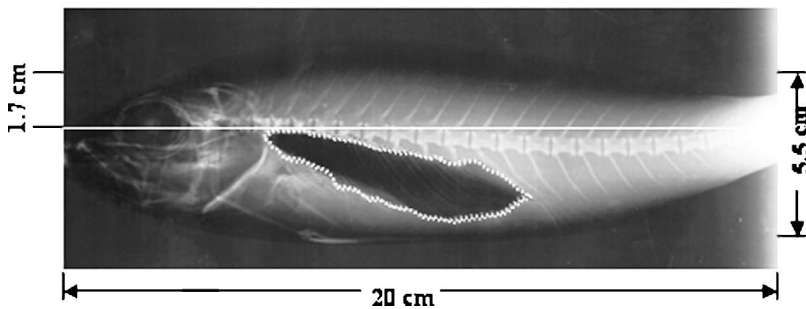


FIG. 7. An expanded plot of the envelope of the cross-correlation function of Fig. 4 for the pink snapper, along with the time delay between each highlight and the first highlight at 0° . The inserted table indicates the delay time and the corresponding two travel distances from the first highlight at 0° . The large differences between the two travel distances and the dimensions of the fish in the x ray indicate a very complex back-scattering process.



distinguish differences in spectral structure that are caused by species differences in the shape of the swimbladder, a relatively small structure.

In order to observe the relationship between highlight spacing and the ripple structure in the spectral domain, consider a target that produces an echo, $e(t)$ with n distinct and separable highlights that can be expressed as

$$e(t) = a_0s(t) + a_1s(t - \tau_1) + \dots + a_ns(t - \tau_n), \quad (4)$$

where a_n is the amplitude of the n th highlight and τ_n is the delay time between the n th highlight and the first highlight. The spectrum of Eq. (4) can be expressed as

$$|E(f)| = |S(f)| \{ [a_0 + a_1 \cos(2\pi f\tau_1) + \dots + \cos(2\pi f\tau_n)] + [a_1 \sin(2\pi f\tau_1) + \dots + \sin(2\pi f\tau_n)] \}^{1/2}. \quad (5)$$

The cos and sin terms are responsible for the ripple pattern and the τ term specifies the position of the nulls in the spectrum. From Eq. (5) we can obtain an insight between the relationship of the spectra shape and highlight intervals.

Fish size is traditionally related to target strength. The relationship between fish length and target strength for the snapper species was not particularly strong (Benoit-Bird *et al.*, 2003a). Fish length was also indicated by the time and frequency characteristics of broadband echoes. The distance between highlights in each species generally increased with fish standard length. The frequency of spectral peaks and nulls generally decreased with increasing fish length. Highlight width was not correlated with fish size. The use of the combination of these factors correlated with fish length, in-

cluding temporal and spectral structure and target strength, could provide a more accurate estimate of fish length. This combination of factors could also provide an error term for each individual fish instead of one error estimate for all fish measured.

The position of spectral characters was correlated with fish length within each species. Dividing fish length by the frequency of the individual character should remove the effect of length. In other words, the length of the fish divided by the wavelength of the spectral character should be a constant with no correlation with fish length. However, this does not occur for any spectral characteristic in any of the three species. Utilizing the size characteristics of the swimbladder instead of fish length did remove the effect of fish size, however. This indicates the importance of the swimbladder not only in the amplitude of the echo, but in its spectral characteristics. Interestingly, none of the spectral characteristics of the echoes appear to be caused by the remainder of the body of the fish.

The structure of the broadband echoes cannot be solely explained by specular reflections off different parts of the swimbladder. That the echo structure is related to the swimbladder shape can be surmised by considering the shapes shown in Fig. 4 of Benoit-Bird *et al.* (2003a) and the time waveforms in Fig. 2. Each of the snapper species had different swimbladder shapes and, subsequently, differences in the backscatter waveforms. Some of the echoes had durations of over 400 μ s, considerably longer than the 80- μ s duration of the incident signal. These echoes suggest the presence of some type of high-frequency resonance associated with the backscatter from the swimbladders of snappers, and perhaps

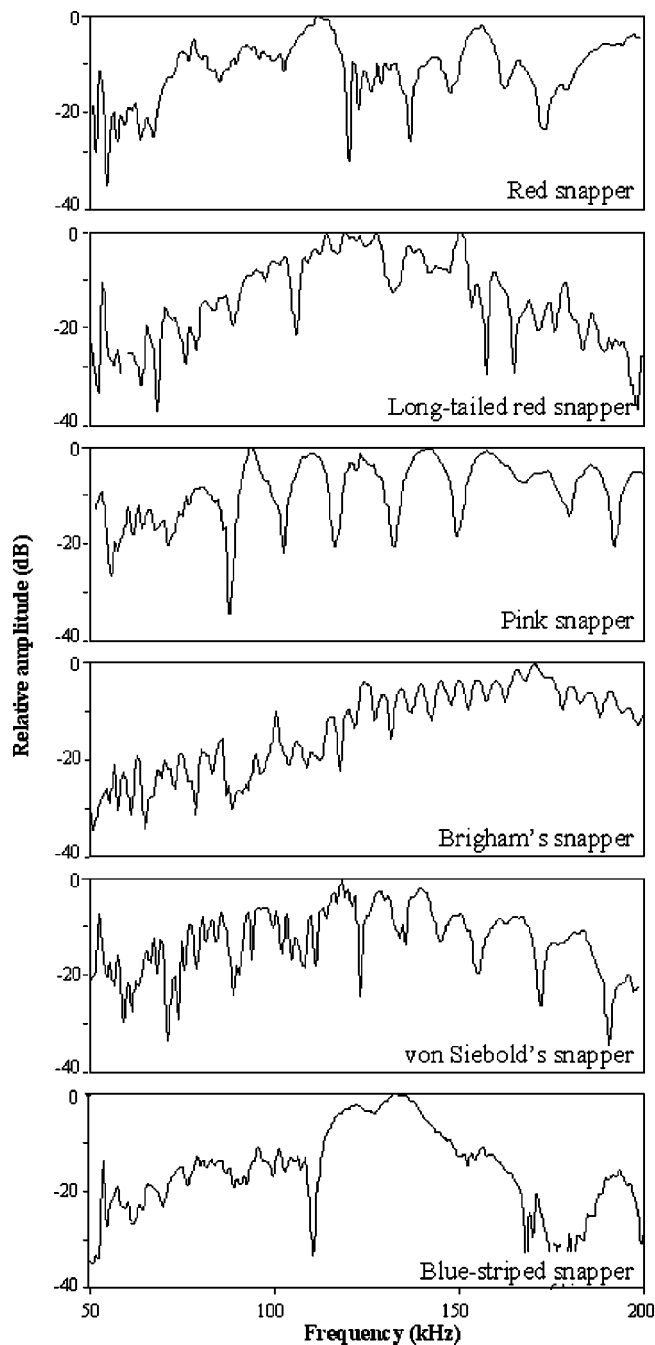


FIG. 8. Representative normalized transfer functions for each of six species of snapper. Echoes are from the broadband, frequency-modulated signal from the dorsal aspect of each fish. Patterns of frequency peaks and nulls were conserved between individuals within each of the three primary species, red, long-tailed red, and pink snapper, regardless of size.

other types of fishes with swimbladders. Echoes from the lateral aspect with the incident signal being perpendicular to the longitudinal axis of the fishes also have relatively long echoes. Examples of echoes from a lateral aspect taken at the surface and *in situ* at 250-m depth using a manned submersible are reproduced from Benoit-Bird *et al.* (2003b) in Fig. 10. The transmitted signal from the sonar on the submersible was the same as the signal used in this study. These echoes illustrate further the complex backscattering process involved with these lutjanid snappers that are not simply explainable at our current level of understanding. The idea of

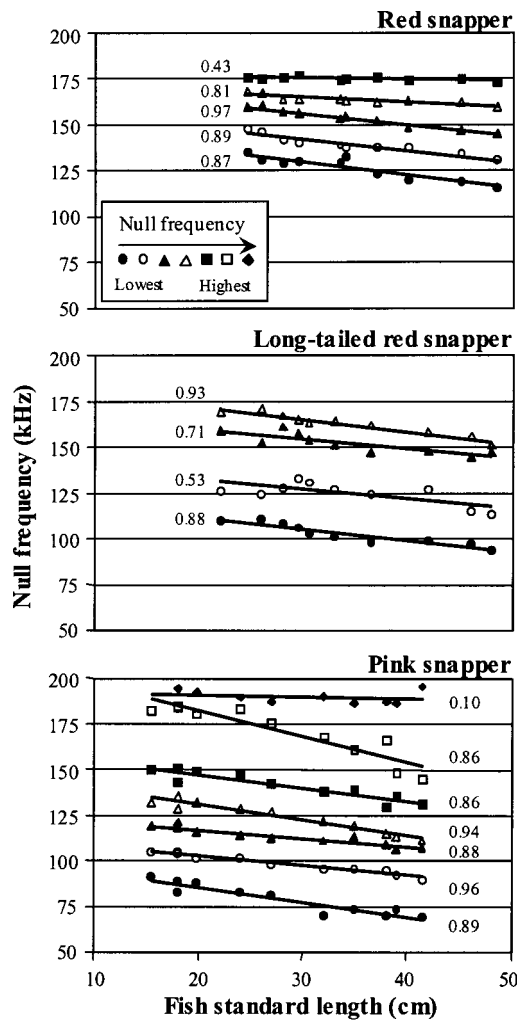


FIG. 9. Frequency of spectral nulls, sharp decreases in amplitude by at least 10 dB, as a function of fish length. Regression coefficients are shown for each relationship. The frequency for each null, except the high-frequency pink snapper null, significantly decreased as fish size increased (F -tests, $p < 0.05$). Similar patterns were observed in frequency peaks.

reflecting waves interacting with various parts of a fish body causing multiple reflections has been considered (Clay, 1991, 1992); however, whether the model used can explain broadband echo durations that are as much as five times longer than the incident signal is questionable. Certainly more physical and mathematical modeling research needs to be done in order to understand the complicated backscatter processes evident in our data.

Fish and their swimbladders are complicated structures that do not lend themselves to simple geometric description. In order to gain a deeper understanding of the acoustic scattering processes in fish, a detailed numerical technique might be necessary. A possible approach is to obtain the three-dimensional geometry of an entire fish body, including the flesh, bones, and swimbladder using x-ray computed tomographic (CT) scans and applying the wave equation to the situation. Jech and Horne (2002) digitized lateral and dorsal radiographs of a fish to construct a three-dimensional representation of the fish body and swimbladder and applied the Kirchhoff-ray mode model (Clay and Horne, 1994) to calculate the acoustic backscatter in three dimensions. The fish

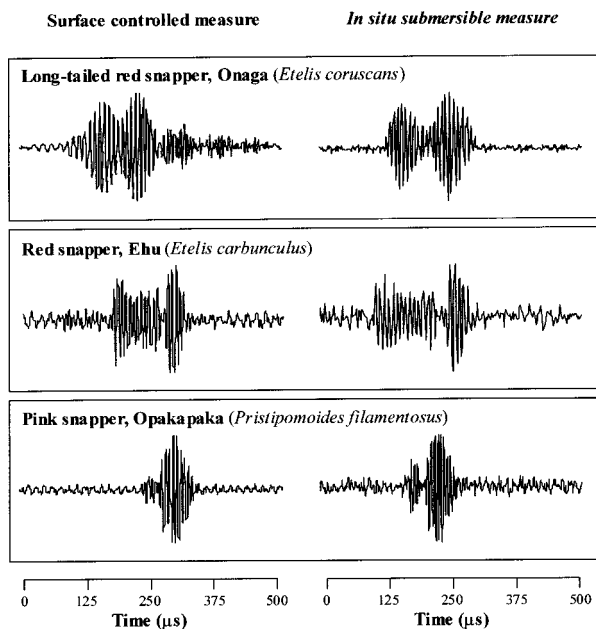


FIG. 10. Representative echoes from the lateral aspect of each Hawaiian snapper species. Echoes on the left were taken from anesthetized fish under controlled conditions at the surface. Echoes on the right were taken from the submersible of free-swimming fish at 250 m.

body and swimbladder were modeled by a series of finite cylinders and the total backscatter was estimated by summing the backscatter overall all the cylinders. Aroyan (2001) has considered the problem of sound propagation in a dolphin's head, modeling the tissue and bones as inhomogeneous fluids so that shear waves could be ignored. He then numerically solved the linearized wave equation using a 3-D finite difference approach. A numerical approach can model the geometry of the backscatter problem more accurately than other approximations using geometry shapes and could also provide a time-history visualization of the scattering process to provide deeper insight into a complex problem. The results obtained by Aroyan were very useful in visualizing in space and time the process of sound propagation and scattering within a complex structure such as a dolphin's head. Whereas Aroyan considered only monochromatic waves, the propagation of a broadband wave such as a pulse would need to be used in order to resolve closely spaced highlights created by fish with many, small internal structures. Much could be learned for such numerical simulation, particularly if species with different swimbladder characteristics are modeled.

ACKNOWLEDGMENTS

Christopher Kelley, Director of the Bottomfish Project, provided support and guidance from the beginning of this work. Aaron Moriwake, Virginia Moriwake, and Bo Alexander maintained the fish while in the hatchery; assisted in the capture of the fish, design of the fish mounting setup, and

data collection; and shared their knowledge and expertise. Kristine Hiltunen, a student in the National Science Foundation's Research Experience for Undergraduates Program, assisted in data collection and processing. Kimberly Andrews assisted in data collection. Christopher Kelley provided helpful comments on earlier versions of this manuscript. This work was supported by the Hawaii State Department of Land and Natural Resources. This is HIMB contribution 1167.

- Aroyan, J. (2001). "Three dimensional modeling of hearing in *Delphinus delphis*," J. Acoust. Soc. Am. **56**, 3305–3318.
- Au, W. W. L. (1993). *The Sonar of Dolphins* (Springer-Verlag, New York).
- Au, W. W. L., and Snyder, K. J. (1980). "Long-range target detection in open waters by an echolocating Atlantic bottlenose dolphin," J. Acoust. Soc. Am. **56**, 1280–1290.
- Barr, R. (2001). "A design study of an acoustic system suitable for differentiating between orange roughy and other New Zealand deep-water species," J. Acoust. Soc. Am. **109**, 164–178.
- Benoit-Bird, K. J., and Au, W. W. L. (2002). "Enersy: Converting from acoustic to biological resource units," J. Acoust. Soc. Am. **96**, 1661–1668.
- Benoit-Bird, K. J., Au, W. W. L., and Kelley, C. D. (2003a). "Acoustic backscattering by Hawaiian lutjanid snappers. I. Target strength and swimbladder characteristics," J. Acoust. Soc. Am. **114**, 2757–2766.
- Benoit-Bird, K. J., Au, W. W. L., Kelley, C. D., and Taylor, C. (2003b). "Acoustic backscattering from deepwater measured in situ from a manned submersible," Deep-Sea Res., Part I **50**, 221–229.
- Brigham, E. O. (1988). *The Fast Fourier Transform and its Applications* (Prentice-Hall, Englewood Cliffs, NJ).
- Burdic, W. S. (1968). *Radar Signal Analysis* (Prentice-Hall, Englewood Cliffs, NJ).
- Clay, C. (1991). "Low-resolution acoustic scattering models: Fluid-filled cylinders and fish with swim bladders," J. Acoust. Soc. Am. **89**, 2168–2179.
- Clay, C. S. (1992). "Composite ray-mode approximations for backscattered sound from gas-filled cylinders and swimbladders," J. Acoust. Soc. Am. **94**, 2173–2180.
- Clay, C. S., and Horne, J. K. (1994). "Acoustic models of fish: The Atlantic cod (*Gadus morhua*)," J. Acoust. Soc. Am. **96**, 1661–1668.
- Foote, K. G., and Ona, E. (1985). "Swimbladder cross sections and acoustic target strengths of 13 pollack and 2 saithe," Fiskeridirektoratets **18**, 1–57.
- Greenlaw, C. F., and Johnson, R. K. (1983). "Multiple-frequency acoustical estimation," Biol. Oceanogr. **2**, 227–252.
- Haight, W. R., Parrish, J. D., and Hayes, T. A. (1993). "Feeding ecology of deepwater lutjanid snappers at Penguin Bank, Hawaii," Proc. Am. Fish. Soc. **122**, 328–347.
- Jech, J. M., and Horne, J. K. (2002). "Three-dimensional visualization of fish morphology and acoustic backscatter," ARLO **3**, 35–40.
- MacLennan, D. N. (1990). "Acoustical measurement of fish abundance," J. Acoust. Soc. Am. **87**, 1–15.
- MacLennan, D. N., and Holliday, D. V. (1996). "Fisheries and plankton acoustics: past, present, and future," ICES J. Mar. Sci. **53**, 513–516.
- MacLennan, D. N., and Simmonds, E. J. (1992). *Fisheries Acoustics* (Chapman and Hall, New York)
- Simmonds, E. J., and MacLennan, D. N. (1996). "Fisheries and Plankton Acoustics," paper presented at the ICES Marine Science Symposia, London.
- Urick, R. J. (1983). *Principles of Underwater Sound* (McGraw-Hill, New York).
- Western Pacific Regional Fisheries Management Council (1999). "Bottomfish and Seamount Groundfish of the Western Pacific Region, 1998," Annual Report.
- Zakharia, M., Magand, F., Hetroit, F., and Diner, N. (1996). "Wideband sounder for fish species identification at sea," ICES J. Mar. Sci. **53**, 203–208.